

Infrared Imaging of Subcutaneous Veins

Vladimir P. Zharov, PhD,^{1*} Scott Ferguson,¹ John F. Eidt, MD,² Paul C. Howard, PhD,³ Louis M. Fink, MD,⁴ and Milton Waner, MD⁵

¹Philips Classic Laser Biomedical Laboratory, University of Arkansas for Medical Sciences, Little Rock, Arkansas, 72205-7199

²Division of Vascular and General Surgery, University of Arkansas for Medical Sciences, Little Rock, Arkansas, 72205-7199

³National Toxicology Program Center for Phototoxicology, National Center for Toxicological Research (NCTR), U.S. Food & Drug Administration, Jefferson, Arkansas

⁴Central Arkansas Veterans Healthcare System, Little Rock, Arkansas

⁵Arkansas Children's Hospital, Little Rock, Arkansas

Background and Objectives: Imaging of subcutaneous veins is important in many applications, such as gaining venous access and vascular surgery. Despite a long history of medical infrared (IR) photography and imaging, this technique is not widely used for this purpose. Here we revisited and explored the capability of near-IR imaging to visualize subcutaneous structures, with a focus on diagnostics of superficial veins.

Study Design/Materials and Methods: An IR device comprising a head-mounted IR LED array (880 nm), a small conventional CCD camera (Toshiba Ik-mui, Tokyo, Japan), virtual-reality optics, polarizers, filters, and diffusers was used in vivo to obtain images of different subcutaneous structures. The same device was used to estimate the IR image quality as a function of wavelength produced by a tunable xenon lamp-based monochromator in the range of 500–1,000 nm and continuous-wave Nd:YAG (1.06 μ m) and diode (805 nm) lasers.

Results: The various modes of optical illumination were compared in vivo. Contrast of the IR images in the reflectance mode was measured in the near-IR spectral range of 650–1,060 nm. Using the LED array, various IR images were obtained in vivo, including images of vein structure in a pigmented, fatty forearm, varicose leg veins, and vascular lesions of the tongue.

Conclusion: Imaging in the near-IR range (880–930 nm) provides relatively good contrast of subcutaneous veins, underscoring its value for diagnosis. This technique has the potential for the diagnosis of varicose veins with a diameter of 0.5–2 mm at a depth of 1–3 mm, guidance of venous access, podiatry, phlebotomy, injection sclerotherapy, and control of laser interstitial therapy. *Lasers Surg. Med.* 34:56–61, 2004. © 2004 Wiley-Liss, Inc.

Key words: infrared imaging; subcutaneous veins; diagnosis; vascular pathology

INTRODUCTION

The most fundamental procedure in modern emergency medicine is gaining rapid venous access in situations where the condition of the patient precluded successful cannula-

tion to administer fluids, medications, anesthetics, and blood infusions. The extent of difficulty in cannulating a vein depends on several factors, including vein depth, amount of fatty tissue, skin pigmentation, and blood volume. These factors can make finding veins with the naked eye difficult or impossible. In particular, infants are among the most difficult to cannulate since their veins are small in diameter and can be obscured by a healthy covering of fatty tissue.

In some cases, ultrasound can be used to find veins, but the veins must be relatively large [1]. In addition, ultrasound is not universally available and requires considerable expertise to obtain useful images while simultaneously cannulating the vein. Transillumination (light directed from behind the vein) in the visible-light range has been used to improve visualization of veins and has been shown to be somewhat helpful [2]. Still, results with this technique have not been consistent, and in some cases the high intensity of light needed has caused burns. Infrared imaging (IRI) may offer a solution to visualizing veins since IR light penetrates human tissue much better than visible light [3]. Additionally, blood absorbs IR energy to a greater degree than surrounding tissue (e.g., fat or melanin), resulting in high-contrast imaging. Despite a long history of medical IR photography, this technique is not widely used in medicine because of time considerations [3–10]. Prior experiments provided some interesting data using other near-IR detectors [11–20,28–31]. However, the device parameters were empirically selected without detailed experimental studies leaving the clinical prospects unclear. In view of the increased resolution and sensitivity offered by modern electro-optic technologies, including LED-based

*Correspondence to: Vladimir P. Zharov, PhD, Philips Classic Laser Biomedical Lab, University of Arkansas for Medical Sciences (UAMS), 4301, West Markham St., Slot 543, Little Rock, AR 72205-7199. E-mail: ZharovVladimirP@uams.edu

SF has disclosed a potential financial conflict of interest with this study.

Accepted 13 October 2003
Published online in Wiley InterScience
(www.interscience.wiley.com).
DOI 10.1002/lsm.10248

optical sources and advanced CCD cameras, we recently revisited the capabilities of IR imaging and have presented preliminary data at conferences [32,33]. Here we describe further development of this technique with a focus on its capabilities for imaging veins.

MATERIALS AND METHODS

The main goal of the study was to test the hypothesis that IR imagery optimized for venous visualization could offer potential solutions for clinical situations that are known to be difficult.

To realize this goal, we performed experiments *in vivo* with an IR device optimized for imagery of invisible or difficult to see veins encountered by experienced phlebectomist.

Experimental Setup

The general optical scheme of the IR device for imaging venous structures consisted of an illumination source, a diffuser, polarizers, an IR filter, a CCD camera, a video processor, and a monitor (Fig. 1). We used the following optical sources: Nd:YAG laser (CL-MD, Surgical Laser Technologies, Inc., Montgomeryville, PA) producing 1,064-nm light, diode laser (25 W, Diomed Ltd., Cambridge, UK) producing 805-nm light, IR LED array producing 880-nm light, and a 300-W xenon monochromator providing light in the range of 500–1,000 nm with a spectral width of 20 nm. Surface irradiance at the sample ranged from 1 to 100 mW/cm². Ground-glass and holographic diffusers were used with the LED array to produce a smooth illumination intensity distribution. A long-pass IR filter was used to exclude ambient light. Two types of CCD cameras were used: a conventional type for obtaining images in the spectral range of 500–920 nm (MTI Dage CCD72) and a InGaAs lead sulfide camera for imaging in the range of 900–1100 nm. Image contrast was enhanced using signal processing (CE 3000; DigiVision, Inc., San Diego, CA). The output of the real-time contrast enhancer was then displayed on a CRT monitor or a head-mounted display (Glasstron; Sony, Inc.). Additionally, the images were captured with a computer and frame grabber and/or videotape recorder for analysis.

RESULTS

The experiments *in vivo* using volunteers' hands revealed that the optical properties varied significantly

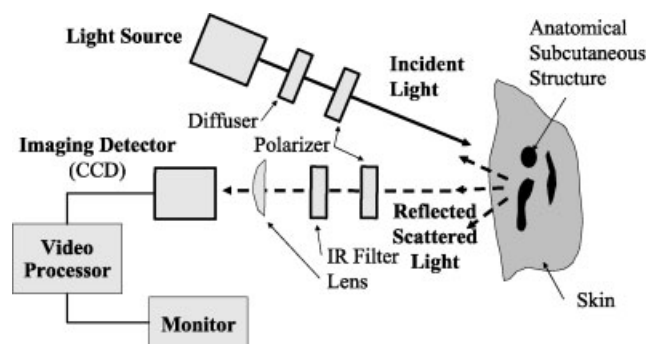


Fig. 1. Schematic diagram of the IR imaging system.

among individuals. For example, the total scattered reflectance (total energy emitted from an irradiated surface) for skin type I (Fitzpatrick) ranged from 45% to 60% at 880 nm, whereas type IV skin ranged from 30% to 40%. It is known [21–27] that specular and diffusive reflections from the surface and the region above a target combine to act as a major source of optical noise during IR reflectance imaging. The efficacy of several methods for reducing surface reflections was compared. The first method involved placing various liquids (water, glycerin, etc.) on the skin in an effort to improve the matching of the index of refraction interface between air and skin. The second method involved increasing the angle of incidence of the illumination source to direct the specular reflections away from the CCD camera. Finally, polarizers were used with varying planes of orientation, as described previously [25,26]. Despite some reduction of surface reflections with the first two methods, neither method offered significant improvement (3–5%), whereas the polarizers reduced surface reflections by as much as 7–8%. The best arrangement for minimizing surface reflections was found to occur using polarizer, oriented perpendicular to each other and light, directed to the target 30° relative to normal. This scheme allows imagery of randomly polarized light returning from the deep tissue while rejecting the specular-superficial reflections known to preserve polarization [25].

A qualitative comparison of IR images produced using three different modes of illumination is presented in Figure 2. The left image demonstrates the results obtained using the aforementioned illumination scheme with an 880-nm LED array as the source. This wavelength was selected since it is close to the region of maximum spectral contrast, as will be shown later. The CCD camera and the LED array were placed together at a distance of 50 cm from the object. The second IR image (center) demonstrates the results obtained using a dual illumination approach. In addition to the directional illumination used in the prior image, quasi-transillumination was added. This was accomplished using a dual fiber optic-coupled halogen lamp placed on each side of the forearm. Barriers were used to shield the camera from direct illumination produced at the fiber-tissue interface. The final IR image in Figure 2 was obtained using the same illumination technique as the first but using higher irradiance. The first array was replaced with an array comprised of twenty high-output 875-nm LEDs arranged in a parabolic orientation. The light was projected onto the hand using a collection lens, which produced a 85 mm × 30 mm spot. Clearly, the arrangements used to produce the second and especially the third images provided the best contrast.

The spectral study of venous contrast associated with IR imagery *in vivo* was accomplished using volunteers with type I skin (Fig. 3). The region between the wrist and the elbow was imaged, as shown in Figure 2. The average depth of the veins was approximately 1.5–2 mm with an average diameter of 1–2 mm. These data were obtained by pulling the skin, containing the target vein, away from the arm then transilluminating to increase contrast. The depth of relatively large veins were obtained using conventional

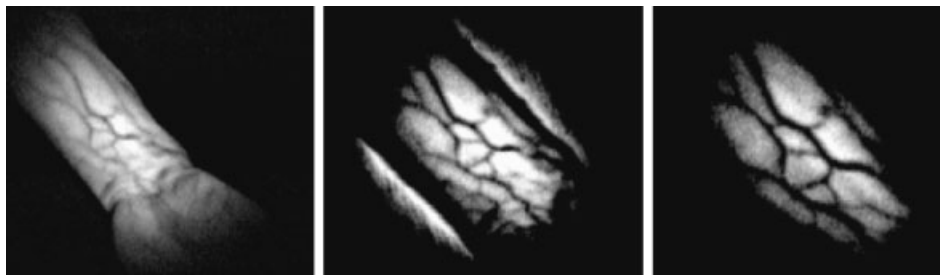


Fig. 2. Enhancement of IR images of a white hand in night conditions with different methods of illumination: **left**, conventional reflectance mode; **center**, combined reflectance–transillumination mode; **right**, local illumination with spatial filtration.

high frequency US techniques [1]. A conventional CCD camera was used to study wavelengths less than 930 nm. An IR CCD camera was used for wavelengths greater than 900 nm. Greater illumination intensity was required beyond 1,000 nm and the Nd:YAG laser were used for this purpose. Image contrast was empirically estimated as the ratio of image intensity in the area immediately adjacent to the imaged vein (bright spot), to the intensity of the imaged vein (dark spot). Quantitative measurements of absolute contrast were difficult to obtain due to the combined effects of scattered light and the irregular nature of the images. However, there are several observations that can be made concerning the contrast. First, there is a slight wavelength-dependence on the magnitude of the contrast. Secondly, for deeper veins, contrast was reduced as the illumination wavelength was decreased while superficial venous contrast was relatively unaffected throughout the studied spectral range. Finally, 570–590 nm appeared to produce the maximum contrast for superficial veins (not shown). We tested the IR imager to assess its capabilities in the following areas: locating veins in adult forearms, pediatric cannulation, diagnostics of venous leg pathologies, and laser interstitial therapy (LIT) control.

IR Imaging of Forearms

Figure 4 shows the IR device, resting on monitor, imaging a forearm in the foreground. The IR device comprised an

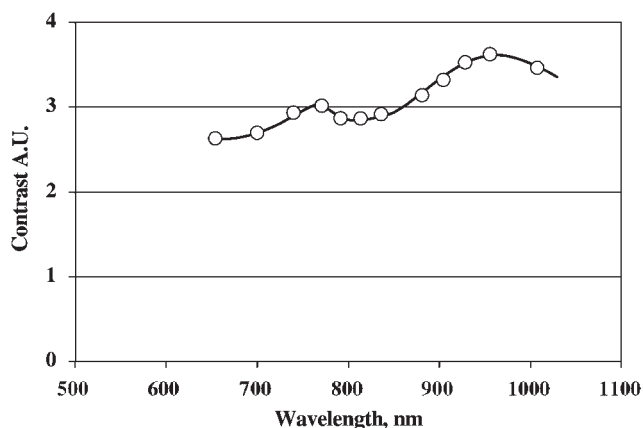


Fig. 3. Relative contrast of IR images in vivo as a function of wavelength.

LED array (880 nm), a compact conventional CCD camera (Toshiba IK-M41) and a liquid crystal display—all mounted onto a comfortable headband similar to that used for head-mounted surgical lights. The image on the monitor is typical of the performance offered by this arrangement. The image is simultaneously displayed on the head-mounted LCD display as well. Figure 5 demonstrates IR imaging (IR image superimposed on white light image) of a traditionally difficult subject. The high melanin concentration (African-American volunteer, Fitzpatrick skin type V) combined with layers of lipid cells created poor white light visualization conditions. The use of IR light (880 nm), however, reduced the absorption by melanin and the scattering of light in the superficial skin layers. Contrast is not as good as that seen in Figure 2, but is sufficient for visualizing veins at an estimated depth of 3–4 mm.

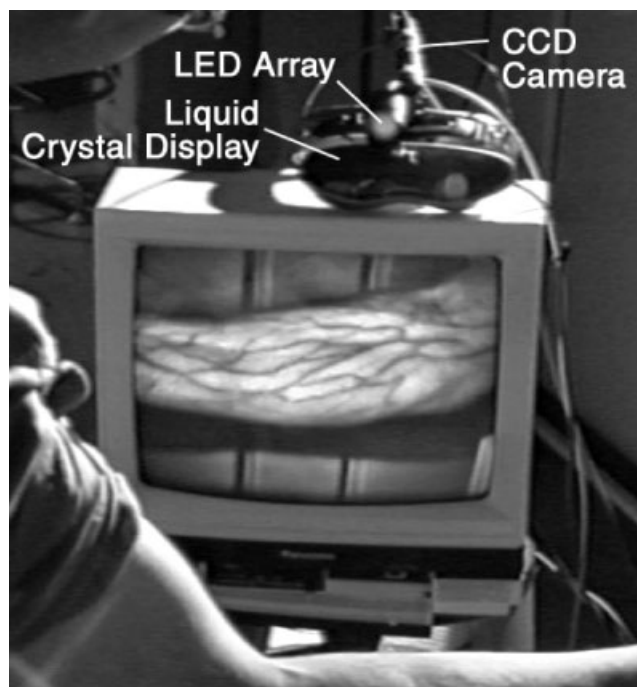


Fig. 4. Monitor screen showing an IR image of a hand. The IR device is located on top of the monitor.

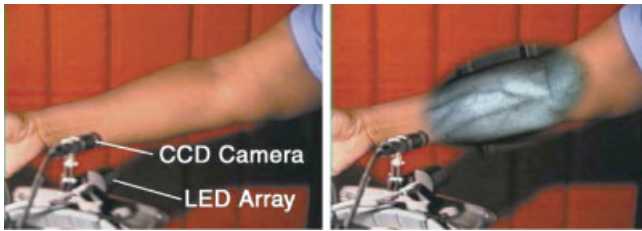


Fig. 5. Comparison of conventional (**left**) and IR (**right**) images (oval black-and-white area) of a fatty, melanin pigmented arm.

IR Imaging of Varicose Veins

We have used an IR imaging system to visualize venous structures ranging in sizes from telangiectasis to larger reticular veins. The system comprised an IR-producing lamp, a video camera, an infrared filter to eliminate visible light, a video signal processor, and a monitor as described previously. With the patient in the upright position, the leg is illuminated with the IR light source, and the image is displayed on the monitor. Figure 6 shows images obtained with a conventional camera (**left**) and the IR system (**right**). Clearly, some venous pathology that is hardly distinguishable by conventional means is obvious with IR imaging. This technique could be useful for locating appropriate injection sites during sclerotherapy or for preoperative mapping. The dark spot seen in both images is used for location reference.

Guidance of Laser Interstitial Therapy (LIT)

The IRI device was used to monitor a LIT treatment to determine if it could provide useful information for control purposes. Figure 7 shows the images obtained during the treatment (diode laser, 805 nm, 2 W, 180 seconds) of a vascular lesion within the tongue. The preliminary results demonstrated that the IRI could help to establish the



Fig. 6. IR imaging for diagnosis of leg vein pathology (varicosity). **Left**, conventional color image in the visible-light range; **right**, IR image for guidance of lower limb phlebotomy.

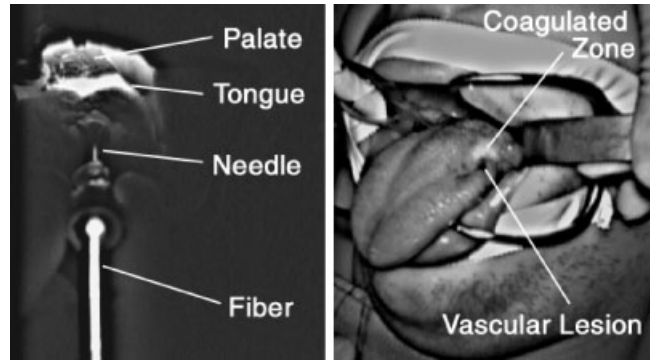


Fig. 7. IR imaging of tongue vascular pathology. **Left**, visualization of laser radiation during LIT; **right**, IR image of margin of laser-treated (coagulated) zone.

approximate location of the distal end of the fiber, around 6 mm, within the tissue. Relatively high output power from the treatment, combined with scattering, compromised the accuracy of this estimate. However, we feel that a low (pilot) power setting could be used prior to treatment to improve the accuracy of this estimation. This information could be used not only to improve treatment accuracy but also avoid morbidity associated with improper fiber placement. In addition to localization information, the image intensity profile provided by the IRI changed during the treatment. This effect was probably due to photothermal alterations within the tissue. Further studies should be conducted to determine how this information could be used for real-time treatment monitoring. Finally, the device provided information as to the margins of the laser-induced coagulation as seen in the right photo of Figure 7.

DISCUSSION

Reports in the literature underscore that, in general, IR image quality depends on many parameters including; light source type, wavelength, and signal processing [11–31]. Many questions remain, however, with no clear answer to issues such as the optimal spectral region or optical scheme. Our studies have focused on three main areas of importance: imaging depth, optimal spectral range, and illumination techniques for venous imagery.

Imaging Depth

Although depth of penetration, L_P , is greater in the IR than in the visible plays a significant role in imaging deep structures, other parameters such as transport mean free paths, L_F , may also contribute significantly to the imaging process [22–24]. The optical properties for skin in the 700–900 nm range are $L_F \sim 1\text{--}3$ mm and a corresponding L_P of $\sim 4\text{--}8$ mm [20–25]. Thus, despite relatively deep penetration, quantitative data and clear images of small objects with sizes D , for which $D < L_F$, can only be obtained within a few millimeters of depth. This correlates well with our good visualization of 0.5–1.5-mm diameter veins that were less than 3 mm below the skin's surface (Figs. 2, 4, and 5).

Optimal Spectral Range

In the optical window of 700–1,000 nm, tissue is a highly scattering medium and more light will be redistributed within the volume than is absorbed by it. The best optical contrast (determined by the absorption coefficient ratio of the veins and surrounding tissues) is expected to be in the visible range near the maximum absorption of hemoglobin [22]. This is valid for veins located near the surface with just a very thin layer of melanin. With increased depth, however, tissue absorption and scattering prevent the formation of clear vascular images using visible light. The maximum contrast in this situation will shift towards the IR range where tissue scattering and absorption decreases while hemoglobin absorption within the veins remains sufficient to provide significant contrast. The data illustrated in Figure 3 demonstrate, however, that for veins at depths of 1–3 mm, wavelength is not critical for contrast. This observation can be explained by the approximately monotonic decreases in melanin and hemoglobin absorption as wavelength increases. In the near-IR range, oxyhemoglobin, has a relatively broad maximum extending into the longer wavelengths at 830–950 nm. Thus, experimental results (Fig. 3) demonstrate that the maximum contrast occurs at approximately 920 nm, as would be expected. From a practical point of view, a typical monochromatic CCD camera's spectral sensitivity at 940–960 nm is approximately 8–10 times less than within the visible range. In the longer-IR range it is necessary to use special IR cameras which are relatively large, expensive, and exhibit lower sensitivity. Thus, a compromise was made between cost and image quality in the spectral range of 880–900 nm.

Reflectance Versus Transillumination Modes

The third important issue relates to the various illumination techniques for venous imagery. In the direct illumination mode, specular reflections from the surface and scattering events in the space between the irradiated skin surface and the vein produce significant optical noise. The image is formed by preferential venous absorption within a scattering media. The scattered photons that return to the camera register the venous images as shadows. Our experimental data revealed that for veins in which $D < L_F$ (i.e., around 0.5–1 mm) scattering events significantly degraded image contrast, where as larger veins with sizes $D > L_F$ (i.e., > 1 mm) only the margins were partially affected. In the transmission, or bright field mode, the target is illuminated by photons emanating primarily from the background. As the light proceeds through the tissue, venous absorption blocks the light and provides excellent contrast imagery. The improved contrast can be explained by the reduction of scattering that occurs in the space between the vessel and surface when compared to the direct illumination technique. The significant advantage of bright field illumination is that it provides excellent contrast imagery of veins beyond the reach, depthwise, of direct illumination. However, this technique is limited by sample thickness and power density. To image thick regions, more light is required, but is limited by the thermal damage threshold of skin. The advantage of direct

illumination is that imagery can occur on any portion of the body. The drawbacks of this technique are limited imaging depth and reflection/scatter induced foreground optical noise. We found that by using a very smooth light-intensity distribution, we could increase contrast and distinguish minor intensity variations. For this purpose, we used a holographic diffuser located in front of the LED sources. We also found that contrast improved as the illumination spot size was decreased. These findings can be attributed to the influence of photons captured outside the region of interest, which primarily consist of optical noise. Thus, with the use of a narrow illumination beam and increased magnification, the analog "spatial filtration" significantly increased contrast (Fig. 2, right). As a compromise between the two modes of operation, a quasi-transillumination dark field method was tested in combination with direct illumination. The testing of different parameters (incident angle, light spot size, location of irradiated area, etc.) revealed that the best results were obtained using multiple points of illumination adjacent to the vein being imaged. The illumination was provided by a fiber optic pressed into the tissue approximately 1–2 cm from the vessel. To exclude of the strong influence of scattered photons emitted from the skin close to the irradiated area, we used shields around the fibers. As results of all these efforts, reasonably good venous contrast was obtained (Fig. 2, center). Thus, by manipulating the wavelength, illumination geometry, and filtration, sufficient contrast was obtained to visualize deeper veins (Fig. 5).

The significance of venous images of the leg must be judged in conjunction with physical examination and duplex ultrasound. The IR system can be used preoperatively to visualize the location and the size of varicose veins before ambulatory treatment (phlebectomy). Precise preoperative mapping can markedly increase the effectiveness of ambulatory phlebectomy and reduce the risk of recurrence. Compared to duplex ultrasound, the IR technique allows visualization of relatively small reticular veins that may be both symptomatic and unsightly.

With careful study, application of this IR technology may also improve the efficacy and the safety of LIT. It may also improve fiber placement accuracy and provide laser dosimetry feedback during LIT. Although the use of IR imaging to determine the margin of coagulation is still at a very preliminary stage, it is our hope that additional study will make IR imaging useful for wound management of burn victims without the use of contrast agents.

Other Applications

Another area of potential use for IR imaging is the visualization of superficial tumors accompanied by vascular abnormalities. Recently, we have demonstrated in the frame collaboration with NCTR (Dr. P. Howard) that the IR technique may be used in combination with visible light for imaging superficial UV-induced tumors (squamous cell carcinoma) in vivo using animal models. The resolution and contrast of small superficial veins can be increased by combining IRI with microscopy and was demonstrated during the examination of some pathologies in the oral

cavity. These included microvascular abnormalities in the mucosa, teeth stone, caries of the teeth, and inflammation around implants [34]. IR imaging provided well-contrasted images of (Fig. 7, right) of hair follicles. In some instances, when high magnification was implemented, images down to the dermal papilla were obtained. These capabilities make IR imaging a promising technique for controlling cosmetic hair removal procedures. In an effort to further develop the IR imaging technique, a three-dimensional version was developed. A loss of depth perception was identified as a potential weakness of the instrument. This limitation was addressed using two CCDs, separated by the typical interpupillary distance, each feeding video into the separate channels of a stereo head-mounted display. This preliminary study revealed that spatial information could be provided for dexterity concerns.

CONCLUSION

Despite significant progress in the development of new, advanced imaging techniques, such as time and frequency domain methods, optical coherence tomography, and others, our findings confirm that relatively old and simpler IR imaging techniques combined with some improvements and modern technological implementation offer a promising approach to diagnostics of subcutaneous venous structures. In general, our investigations have revealed that IR imaging can visualize vascular structures with a minimum diameter of ~ 0.2 mm within 0.5–1 mm of the skin's surface and veins with a diameter of 1–2 mm down to 3–4 mm. The data we presented show promise for introducing this technique into many areas of medicine, including diagnosis of venous leg pathologies, phlebectomy, vascular surgery, catheter localization, and guidance of various surgical interventions such as LIT.

REFERENCES

- Donaldson JS, Morello FP, Junewick JJ, O'Donovan JC, Lim-Dunham J. Peripheral inserted central venous catheters: US-guided vascular access in pediatric patients. *Radiology* 1995; 197:542–544.
- Weiss HL, Goldman MP. Transillumination mapping prior to ambulatory phlebectomy. *Dermatol Surg* 1998;24:447–450.
- Haxthausen H. Infrared photography of subcutaneous veins: Demonstration of concealed varices in ulcer and eczema of the leg. *Br J Dermatol* 1933;45:506–511.
- Henderson JW. Infrared photography revisited. *J Audio Media Med* 1993;16:158–162.
- Kodak E. Medical infrared photography. Rochester, NY: Eastman Kodak Co; 1969.
- Ford RJ. Infrared photography of transilluminated infant skulls. *J Biol Photogr Assoc* 1974;42:94–102.
- Marshall RJ. Infrared and ultraviolet photography in a study of the selective absorption of radiation by pigmented lesions of skin. *Med Biol Illus* 1976;26:71–84.
- Poliakov VA, Volodin AN, Zhuravlev IV. Photographing in infrared and ultraviolet light as a method of determining the viability of injured tissues. *Voen Med Zh* 1981:39–42.
- Moore JW, DeWolf AR, Mitnick MB. Infrared photography: A possible research technique in podiatric medicine. *J Am Podiatry Assoc* 1978;68:53–55.
- Stevenson J. Penetration of eschar by infrared photography. *J Audio Media Med* 1981;4:141–143.
- Hintz SR, Cheong WF, van Houten JP, Stevenson DK, Benaron DA. Bedside imaging of intracranial hemorrhage in the neonate using light: Comparison with ultrasound, computed tomography, and magnetic resonance imaging. *Pediatr Res* 1999;45:54–59.
- Bale M. High-resolution infrared technology for soft-tissue injury detection. *IEEE Eng Med Biol Mag* 1998;17:56–59.
- Mansfield JR, Sowa MG, Scarth GB, Somorjai RL, Mantsch HH. Fuzzy C-means clustering and principal component analysis of time series from near-infrared imaging of forearm ischemia. *Comput Med Imaging Graph* 1997;21:299–308.
- Robertson CS, Gopinath SP, Chance B. A new application for near-infrared spectroscopy: Detection of delayed intracranial hematomas after head injury. *J Neurotrauma* 1995;12:591–600.
- Gostout CJ, Jacques SL. Infrared video imaging of subsurface vessels: A feasibility study for the endoscopic management of gastrointestinal bleeding. *Gastrointest Endosc* 1995;41:218–224.
- Jones CH, Newbery SP. Visualization of superficial vasculature using a Vidicon camera tube with silicon target. *Br J Radiol* 1977;50:209–210.
- Afromowitz MA, Callis JB, Heimbach DM, DeSoto LA, Norton MK. Multispectral imaging of burn wounds: A new clinical instrument for evaluating burn depth. *IEEE Trans Biomed Eng* 1988;35:842–850.
- Gratton G, Maier JS, Fabiani M, Mantulin WW, Gratton E. Feasibility of intracranial near-infrared optical scanning. *Psychophysiology* 1994;31:211–215.
- Hayashi N, Kawano S, Tsuji S, Tsujii M, Takai Y, Nagano K, Fusamoto H, Sato R, Kamada T. Identification and diameter assessment of gastric submucosal vessels using infrared electronic endoscopy. *Endoscopy* 1994;26:686–689.
- Tsuji S, Kawano S, Sato N, Hayashi N, Peng HB, Tsujii M, Nagano K, Takei Y, Chen SS, Kashiviagi T, Fusamoto H, Kamada T. Comparison of infrared electronic endoscopy using reflection and transmission. *Endoscopy* 1993;25:278–281.
- Jarlman O, Berg R, Andersson-Engels S, Svanberg S, Pettersson H. Time-resolved white light transillumination for optical imaging. *Acta Radiol* 1997;38:185–189.
- Farrell TJ, Patterson MS, Wilson B. A diffusion theory model of spatially resolved, steady-state diffuse reflectance for the noninvasive determination of tissue optical properties in vivo. *Med Phys* 1992;19:879–888.
- Patterson MS, Wilson BC, Wyman DR. The propagation of optical radiation in tissue II: Optical properties of tissues and resulting fluence distributions. *Lasers Med Sci* 1991;6:379–390.
- Key H, Davies ER, Jackson PC, Wells PN. Monte Carlo modeling of light propagation in breast tissue. *Phys Med Biol* 1991;36:591–602.
- Anderson RR. Polarized light examination and photography of the skin. *Arch Dermatol* 1991;127:1000–1005.
- Demos SG, Alfano RR. Optical polarization imaging. *Appl Opt* 1997;36:150–155.
- Jacques SL, Ramella-Roman JC, Lee K. Imaging skin pathology with polarized light. *J Biomed Opt* 2002;7:329–340.
- Zeman HD, Lovhoiden G. Enhancing the contrast of subcutaneous veins. *Proc SPIE* 1999;3595:219–230.
- Zeman HD, Lovhoiden G, Deshmukh H. Optimization of subcutaneous vein contrast enhancement. *Proc SPIE* 2000;3911:50–57.
- Zeman HD, Lovhoiden G, Deshmukh H. Design of a clinical vein contrast enhancing projector. *Proc SPIE* 2001;4254:204–215.
- Lovhoiden G, Deshmukh H, Zeman HD. Clinical evaluation of vein contrast enhancement. *Proc SPIE* 2002;4615:61–70.
- Zharov V, Waner M, Ferguson S, Eidt J. Infrared imaging of subcutaneous veins structure. *Lasers Surg Med* 2001;28:64–65.
- Zharov VP, Waner M, Ferguson S. Infrared imaging of subcutaneous structure. *BiOS 2001: International Biomedical Optics Symposium Abstract*. San Jose, CA, 2001, 4 p.
- Spiridonov IN, Zharov VP, Levandovskii A. Infrared imaging of biological tissue in mouse cavity. *Proceeding of International Symposium on Medical Physics*. Moscow oncology center, Russia, 1995, pp 26–27.